CHIN. PHYS. LETT. Vol. 36, No. 7 (2019) 074101

Spatial Characteristics of Thomson Scattering Spectra in Laser and Magnetic Fields *

Li Zhao(赵丽)[1], Zhi-Jing Chen(陈之景)[1], Hai-Bo Sang(桑海波)[1,2], Bai-Song Xie(谢柏松)[1,2]**

[1]*Key Laboratory of Beam Technology of the Ministry of Education, and College of Nuclear Science and Technology, Beijing Normal University, Beijing 100875*

[2]*Beijing Radiation Center, Beijing 100875*

(Received 9 May 2019)

Spatial characteristics of Thomson scattering spectra are studied for an electron moving in the circularly polarized laser field in the presence of a strong uniform magnetic field. The results show that the angular distributions of the spectra with respect to the azimuthal and polar angles exhibit different symmetries, respectively, which depend on the fields and electron parameters sensitively and significantly. Moreover, for relatively large parameters such as high laser intensity, high magnetic resonance parameter as well as large initial momentum of electron, the two lobes in spectra tend to the laser-propagating direction so that the radiation can be collimated in the forward direction. Furthermore, an important finding is that by choosing the appropriate fields and initial momentum of electron, the high frequency part of the Thomson scattering spectra can reach the frequency range of soft x-ray, in which a high radiation power per solid angle as $\sim 10^{11}$ *a.u. can be obtained.*

PACS: 41.60.−m, 42.55.Vc, 42.65.Ky DOI: 10.1088/0256-307X/36/7/074101

In the past decades, many advances and developments have been achieved theoretically as well technically in ultrastrong ultrashort lasers interacting with matter.[1−6] Among them, Thomson scattering is a very important phenomenon, which has a potential application to produce attosecond or even zeptosecond x-ray pulses.[7,8] It has been realized that x-ray generated by Thomson scattering has many advantages such as well-collimation, short duration and high peak brightness. Therefore, the Thomson scattering produced by relativistic electrons in laser or/and magnetic fields has been researched widely in both experiment[9−13] and theory.[14−24]

In experiment, Schwoerer *et al.* observed the Thomson backscatter of electrons accelerated by laser pulses and found the collimated x-ray pulse with keV photon energy and sub-picosecond duration.[9] Recently, high-order multiphoton scattering is measured, in which more than 500 near-infrared laser photons are scattered by a single electron into a single x-ray photon.[13] In addition to x-ray, generation of a narrow divergence, multi-MeV and ultrahigh peak brilliance γ-ray beam from scattering of an ultra-relativistic laser-wake-field accelerated electron beam is also reported.[12] Laser-based x-ray/γ-ray sources that provide sufficient photon numbers in narrow bandwidth spectral lines have been applied as the probing way in many experiments, see Ref. [10] for a detailed review.

In theory, the trajectory and energy equations of the electron in combined laser and magnetic fields are obtained by Salamin and Faisal, and the harmonic generation spectrum is given by the doubly differential cross section.[14,15] Then, the radiation spectra in square sinusoidal laser pulse with a uniform magnetic field are also studied numerically, showing that the forward and backward spectra get richer in the presence of the uniform magnetic field.[16] Later, based on the periodicity of electron's motion, He *et al.* developed a new simplified calculation method which is associated to delta function expression. They obtained the phase dependence of the radiation spectra and some interesting scaling laws in a linearly polarized plane wave laser field.[19−21] By the simplified method, the properties of the Thomson back-scattering spectra are explored concretely in combined magnetic and laser fields, seen in our recent works,[23,24] where the scale invariance and scaling laws of the radiation spectrum with the relevant parameters, such as the laser intensity and the initial axial momentum, are found. In addition to the study of the radiation spectrum, in 2009, the spatial characteristics of the Thomson scattering were studied in a linearly polarized laser field by Lan *et al.*, showing that the symmetry of the angular distributions depends sensitively on the initial phase.[22]

However, the relevant spatial distribution of the Thomson scattering in the case of combined circularly polarized laser and magnetic fields has not been studied so far, and the radiation intensity of the Thomson back-scattering spectra is not high enough to apply. Therefore, in this Letter the spatial characteristics of the Thomson scattering are investigated in detail. Based on the angular distributions, the directions where the radiation is strong are obtained, thus the present study can provide a theoretical reference to promote the application of generated x-ray in the experiments.

We consider the angular distributions of the Thomson scattering when the electron (with mass m and charge $-e$) moves in the simultaneous laser and magnetic fields. The external uniform magnetic field is assumed in strength B_0, while the laser field is a left-

*Supported by the National Natural Science Foundation of China under Grant Nos 11875007 and 11305010.

**Corresponding author. Email: bsxie@bnu.edu.cn

© 2019 Chinese Physical Society and IOP Publishing Ltd

hand circularly polarized plane wave with vector potential amplitude A_0 and frequency ω_0. The laser-propagating direction and the magnetic direction are both along the positive z axis. The phase of the laser field is $\eta = \omega_0 t - \boldsymbol{k}\cdot\boldsymbol{r}$, where $\boldsymbol{k}$ and $\boldsymbol{r}$ are the laser wave vector and electron displacement vector, respectively, and the combined fields can be expressed by the total vector potential

$$\boldsymbol{A} = A_0[-\sin\eta\boldsymbol{i} + \cos\eta\boldsymbol{j}] + B_0 x\boldsymbol{j}. \tag{1}$$

Here time is normalized by $1/\omega_0$, displacement by $1/k_0$, momentum by mc and the magnetic field by $eB_0/m\omega_0 c$. Since an electron moves in a constant-amplitude laser field, we can obtain the constant of the motion as $\varsigma = \gamma - p_z = \gamma_0 - p_{z0}$, where γ is the electron relativistic factor, p_z is axial momentum of electron, and γ_0 and p_{z0} are the initial values of them.

The electron is assumed at $(0, 0, z_{\rm in})$ initially. Then, from the relativistic equations of the electron's motion, the momenta and displacements of electrons can be obtained as

$$p_x = na\{\sin\eta - \sin[\omega_b\eta - (\omega_b - 1)\eta_{\rm in}]\}, \tag{2}$$
$$p_y = na\{-\cos\eta + \cos[\omega_b\eta - (\omega_b - 1)\eta_{\rm in}]\}, \tag{3}$$
$$p_z = (2n^2a^2/\varsigma)\sin^2[(\omega_b - 1)(\eta - \eta_{\rm in})/2] + 1/2\varsigma - \varsigma/2, \tag{4}$$
$$x(\eta) = (na/\varsigma)\{-\cos\eta + (1/\omega_b)\cos[\omega_b\eta - (\omega_b - 1)\eta_{\rm in}] - (1/\omega_b - 1)\cos\eta_{\rm in}\}, \tag{5}$$
$$y(\eta) = (na/\varsigma)\{-\sin\eta + (1/\omega_b)\sin[\omega_b\eta - (\omega_b - 1)\eta_{\rm in}] - (1/\omega_b - 1)\sin\eta_{\rm in}\}, \tag{6}$$
$$z(\eta) = (na/\varsigma)^2\{(\eta - \eta_{\rm in}) - [1/(\omega_b - 1)]\sin[(\omega_b - 1)(\eta - \eta_{\rm in})]\} + [(1 - \varsigma^2)/(2\varsigma^2)](\eta - \eta_{\rm in}), \tag{7}$$

where $n = 1/(\omega_b - 1)$ is the resonance parameter.[25]

The emission power detected far away from the electron along the direction $\boldsymbol{n} = \sin\theta\cos\varphi\boldsymbol{i} + \sin\theta\sin\varphi\boldsymbol{j} + \cos\theta\boldsymbol{k}$ can be calculated by[26]

$$\frac{d^2I}{d\Omega d\omega} = \frac{e^2\omega^2}{4\pi^2 c}|\boldsymbol{n}\times[\boldsymbol{n}\times\boldsymbol{F}(\omega)]|^2, \tag{8}$$
$$\boldsymbol{F}(\omega) = \frac{1}{\varsigma}\int_{-\infty}^{+\infty} d\eta p(\eta)\exp\{i\omega[\eta - \boldsymbol{n}\cdot\boldsymbol{r}(\eta) + z(\eta)]\}. \tag{9}$$

Based on the periodicity of the electron's motion, we can simplify Eq. (9) by an infinite series of delta functions and use the same computing method as that in our previous work[23] to calculate the emission power along any direction. Similarly, the emissions consist of the fundamental frequency $\omega_1 = 2\pi/(T - \boldsymbol{n}\cdot\boldsymbol{r}_0 + z_0)$ and its high order harmonics $m\omega_1$ with m being an integer. Concretely, they are

$$\boldsymbol{F}(\omega) = \frac{1}{\varsigma}\sum_{m=-\infty}^{+\infty}\boldsymbol{F}_m\delta(\omega - m\omega_1), \tag{10}$$
$$\boldsymbol{F}_m = \omega_1\int_{\eta_{\rm in}}^{\eta_{\rm in}+T} d\eta p(\eta)\exp\{im2\pi h(\eta)\}, \tag{11}$$

$$h(\eta) = \frac{\eta - \boldsymbol{n}\cdot\boldsymbol{r}(\eta) + z(\eta)}{T - \boldsymbol{n}\cdot\boldsymbol{r}_0 + z_0}, \tag{12}$$

where $\boldsymbol{r}_0 = (0, 0, z_0) = (0, 0, T[(\frac{na}{\varsigma})^2 + \frac{1}{2}(\frac{1}{\varsigma^2} - 1)])$ is the drift displacement vector of the electron during one period.

In the following the spatial characteristics of the Thomson scattering are researched from two perspectives. One is angular distributions with respect to the azimuthal angle φ, where the polar angle $\theta = \pi/2$. Accordingly, the detected direction $\boldsymbol{n} = (\cos\varphi, \sin\varphi, 0)$, the fundamental frequency $\omega_1 = 2\pi/(2\pi n + z_0)$, and $h(\eta) = [\eta - \cos\varphi x(\eta) - \sin\varphi y(\eta) + z(\eta)]/[2\pi n + z_0]$. The other one is angular distributions with respect to the polar angle θ, where the azimuthal angle $\varphi = 0$. Accordingly, the detected direction $\boldsymbol{n} = (\sin\theta, 0, \cos\theta)$, the fundamental frequency $\omega_1 = 2\pi/[2\pi n + (1 - \cos\theta)z_0]$, and $h(\eta) = [\eta - \sin\theta x(\eta) + (1 - \cos\theta)z(\eta)]/[2\pi n + (1 - \cos\theta)z_0]$. It is worth noting that in numerical simulation, we integrate the frequency ω and finally obtain the radiation energy per second per unit solid angle of the electron as follows:

$$\frac{d^2I}{d\Omega dt} = \frac{e^2}{4\pi^2 c}\frac{1}{\varsigma^2}(m\omega_1)^2|\boldsymbol{n}\times[\boldsymbol{n}\times\boldsymbol{F}_m]|^2. \tag{13}$$

Figure 1 presents the angular distributions of the mth harmonic radiation with respect to the azimuthal angle φ for different m, p_{z0}, a and n. From Figs. 1(a1)–1(a3), it can be seen that for different harmonic orders the angular distributions exhibit different shapes, but the common characteristic is that they are all symmetric with respect to the y axis. Also, the radiations mainly distribute between $\varphi = \pi$ and $\varphi = 2\pi$. As harmonics m increases, the radiation intensity increases about one order of magnitude when m changes from 600 to 1200, while it is in the same order when m is 1200 and 2000. This is consistent with the properties of radiation spectra in our previous works.[23,24] Comparing different curves in Figs. 1(b1)–1(b3) where the parameters are set as $a = 2$, $n = 5$, $m = 1200$, $p_{z0} = 0$, 1 and 3, the twofold symmetry of distribution still exists. It is found that whether the electron is stationary initially would lead to a different distribution of the Thomson scattering. When $p_{z0} = 0$, see Fig. 1(b1), the radiation is mainly distributed in the negative y regime with a symmetry about this axis. However, when $p_{z0} = 1$, it is no longer symmetric with respect to y axis and now the radiations are approximately uniformly distributed in the xy plane.

On the other hand, for a weak laser field, see Fig. 1(c1), the radiations concentrate around the angle of $\varphi = 270°$. With increasing the laser field, the range of radiation distribution is gradually expanding, as shown in Figs. 1(c2) and 1(c3). As you can see from the charts of Figs. 1(c1)–1(d3), the symmetry of radiation distributions would exist no matter what the laser intensity a and the resonance parameter n are when the electron is stationary initially.

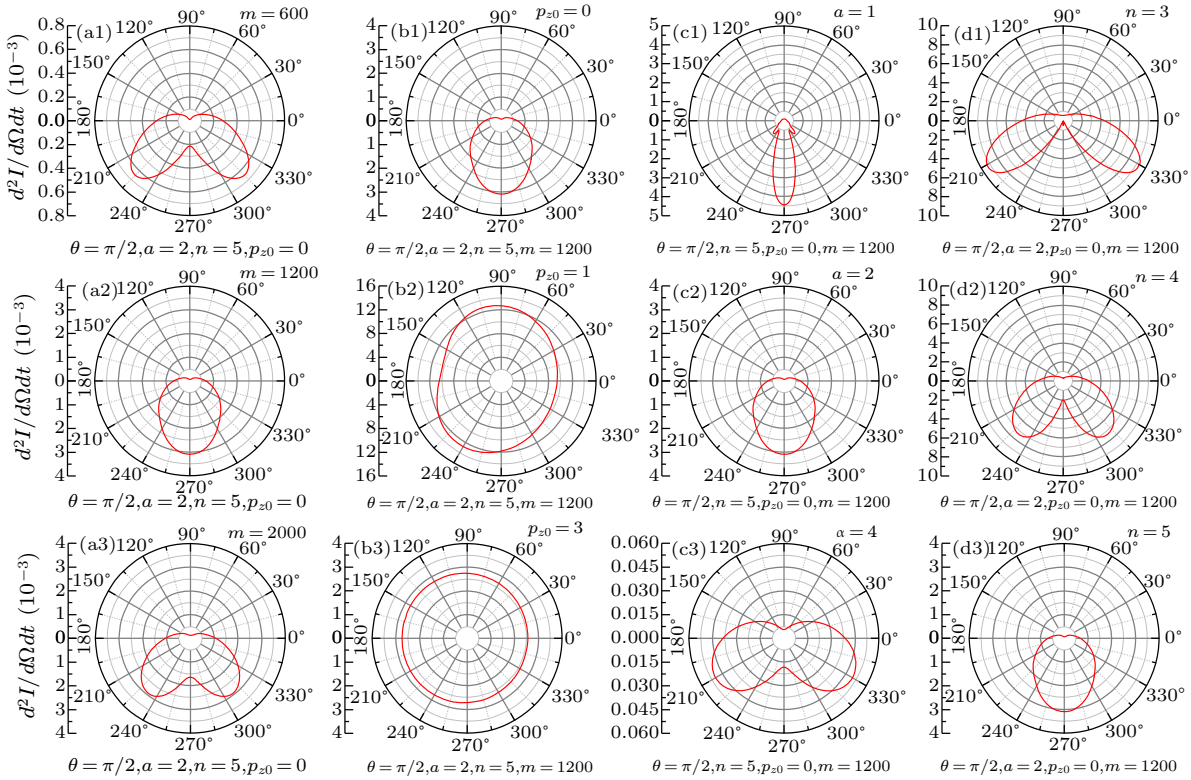

Fig. 1. Angular distributions of the mth harmonic radiation with respect to the azimuthal angle φ with the polar angle $\theta = \pi/2$: (a1)–(a3): $a = 2$, $n = 5$, $p_{z0} = 0$, $m = 600$, 1200 and 2000; (b1)–(b3): $a = 2$, $n = 5$, $m = 1200$, $p_{z0} = 0$, 1 and 3; (c1)–(c3): $n = 5$, $m = 1200$, $p_{z0} = 0$, $a = 1$, 2 and 4; and (d1)–(d3): $a = 2$, $m = 1200$, $p_{z0} = 0$, $n = 3$, 4 and 5.

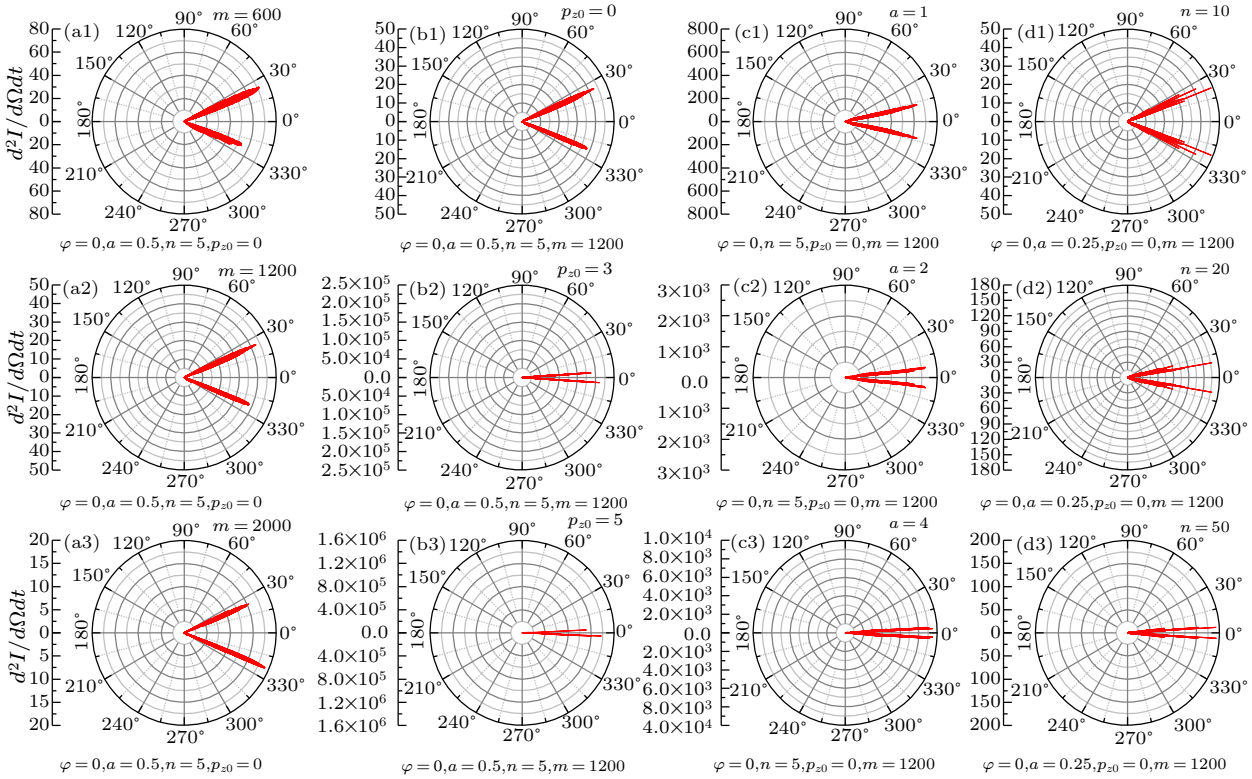

Fig. 2. Angular distributions of the mth harmonic radiation with respect to the polar angle θ with the azimuthal angle $\varphi = 0$: (a1)–(a3): $a = 0.5$, $n = 5$, $p_{z0} = 0$, $m = 600$, 1200 and 2000; (b1)–(b3): $a = 0.5$, $n = 5$, $m = 1200$, $p_{z0} = 0$, 3 and 5; (c1)–(c3): $n = 5$, $m = 1200$, $p_{z0} = 0$, $a = 1$, 2 and 4; and (d1)–(d3): $a = 0.25$, $m = 1200$, $p_{z0} = 0$, $n = 10$, 20 and 50.

Thus in general, the radiation angular distributions with respect to the azimuthal angle φ show twofold symmetry. When the electron is static initially or the laser intensity is small, the strongest radiation is mainly concentrated in a certain angle range. Increasing p_{z0} or a will expand the radiation-distributing range in the xy plane.

Next, let us focus on the angular distributions of the Thomson scattering in the combined laser and magnetic fields with respect to the polar angle θ with the azimuthal angle $\varphi = 0$. As shown in Fig. 2, the angular distribution with respect to the polar angle consists of two lobes collimated in the forward direction. One is in the $+xz$ plane, the other is in the $-xz$ plane. From Figs. 2(a1)–2(a3), we can see that when m increases from 600 to 2000, radiation energy emitted by electron per second per unit solid angle decreases slightly. However, for different harmonic orders, the strong radiations appear at the same polar angles (about 27°), which are axial symmetric of the laser-propagating direction (the z axis), although the distributions in the upper lobe and the lower lobe are not exactly the same.

Figures 2(b1)–2(b3) show the dependence of radiation angular distributions on the initial axial momentum p_{z0}. It is found that with p_{z0} increases from 0 to 3, the radiation intensity increases significantly about 5×10^3 times and the angle between the two lobes gets smaller. Then, comparing (b3) with (b1) and (b2), we find that these two distribution lobes get closer to the laser-propagating direction, which are located at about ±5°. Meanwhile, the dependence of angular distribution on the laser intensity a is also shown in Figs. 2(c1)–2(c3) with the parameters as $n = 5$, $m = 1200$, $p_{z0} = 0$, $a = 1$, 2 and 4. It is obvious that the radiation becomes stronger and stronger with the laser intensity a. If we call the angle of the strongest radiation in upper and lower lobes as $\pm\theta_{\max}$, we can see that with increasing a from 1 to 4, the corresponding $\theta_{\max} \approx 15° \to 7° \to 3°$, i.e., the two lobes get closer to the z axis. Similar to Figs. 2(d1)–2(d3), when the resonance parameter n increases from 10 to 50 with $a = 0.25$, $m = 1200$ and $p_{z0} = 0$, the angle between the two distribution lobes becomes smaller gradually while the radiation intensity decreases.

To sum up, whatever the parameters m, p_{z0}, a and n are, the radiation mainly distributes in two regions, where the angles of the strong radiations $\pm\theta_{\max}$ are well symmetrical with respect to the z axis. Moreover, it is found that the radiation can be collimated in the forward direction when a set of parameters are chosen appropriately.

Table 1. The frequency ω (normalized by ω_0), corresponding radiation energy (normalized by $e^2\omega_0^2/4\pi^2c$) and photon number (normalized by $e^2\omega_0/4\pi^2c\hbar \approx 4\times10^{11}$) per unit solid angle per second for several sets of parameters.

m	p_{z0}	a	n	$\theta_{\max1}$	ω_1	$\omega = m\omega_1$	$(d^2I/d\Omega dt)_{\max}$	$N_{\text{photon}}/d\Omega dt$
1200	0	0.5	5	22.8°	0.1344	1.6125×10^2	4.6292×10^1	2.871×10^{-1}
1200	0	0.25	20	10.6°	0.0350	4.2058×10^1	$8{,}9692\times10^1$	2.1326
1200	0	2	5	7.2°	0.1118	1.3411×10^2	2.6259×10^3	1.9569×10^1
1200	2	0.5	5	6.2°	0.1173	1.4072×10^2	3.4180×10^4	2.4290×10^2
1200	10	0.5	5	1°	0.1415	1.6982×10^2	2.6505×10^6	1.5607×10^4

Finally, we choose several sets of parameters in Fig. 2 and calculate the radiation's frequency, the corresponding radiation energy and photon's number per second per unit solid angle, as listed in Table 1.

Firstly, taking the first-line data as an example, $a = 0.5$, $n = 5$, $p_{z0} = 0$, $m = 1200$, the strongest radiation of upper lobe appears at $\theta_{\max1} = 22.8°$ and the frequency of radiation $\omega/\omega_0 = 1.6125\times10^2$. It means that the radiation's frequency can reach about 10^{17}Hz when the laser whose wavelength $\lambda = 1\,\mu$m is used. The corresponding radiation intensity is about 46.29 (normalized by $e^2\omega_0^2/4\pi^2c$) and the number of radiated photons is about 0.2871, which is normalized by $e^2\omega_0^2/4\pi^2c\hbar\omega_0 = e^2\omega_0/4\pi^2c\hbar \approx 4\times10^{11}$. Therefore, the data in Table 1 indicate that $\sim 10^{10} - 10^{15}$ photons can be emitted by the electron per second per unit solid angle, i.e., the brightness of the beam at the harmonics we cite is good enough to apply in relevant experiments, and the strong radiation of the Thomson scattering can reach the frequency range of soft x-ray with photon energy about hundreds of eV.

In addition, by taking the fifth-line data as another example, $a = 0.5$, $n = 5$, $p_{z0} = 10$, $m = 1200$, when $\lambda = 1\,\mu$m is chosen, the corresponding laser intensity is $I_0 \sim 10^{18}\,\text{W/cm}^2$, the external magnetic strength is $B_0 \approx [(1+1/n)/(2\times p_{z0})]\times100\,\text{MG}\sim600$ tesla, which is available in the present laboratory. Thus under these fields the initial 5 MeV electron can emit $\sim 6\times10^{15}$ soft x-ray photons with ∼170 eV energy per second per unit solid angle. The corresponding radiated power can be estimated as $dP/d\Omega \approx 6.1\times10^{11}$ a.u., which is comparable or/and higher than that seen Fig. 6 in Ref. [13].

Two aspects should be pointed out. One is that our obtained x-ray is about 100 eV, which is smaller than that of some works,[10,13] because we chose the high resonance parameter n. Certainly when the applied magnetic field is strong enough which can reduce n very small then the fundamental frequency ω_1 would be large as the $1/n$ times of the laser frequency so that the m harmonics emission photons would acquire energy of keV or even MeV. This is worthy of further study. However, it is beyond the scope of the present study. On the other hand, here we only consider the Thomson scattering of a single electron but not the electron beam, thus the peak brilliance of the produced soft x-ray is hard to estimate to make comparison with that in experiments.

In summary, the spatial characteristics of the electron's Thomson scattering have been studied in detail

in the combined laser and magnetic fields. Different twofold symmetries are found in the angular distribution with respect to the azimuthal angle φ as well as the polar angle θ. The results also show that the angular distribution is sensitively dependent on the field and electron parameters. In particular, the angle between the two radiation lobes of angular distribution with respect to θ can be reduced ($< 5^\circ$) if we increase the resonance parameter n, the laser intensity a and the initial axial momentum p_{z0}. It is possible that radiation can be collimated in the forward direction with some sets of parameters appropriately. Finally, it is indicated that the high frequency part of the radiation can reach the frequency range of soft x-ray with a high radiated power per solid angle as $\sim 10^{11}$ a.u.

The computation was carried out at the HSCC of the Beijing Normal University.

References

[1] Perry M D and Mourou G A 1994 *Science* **264** 917
[2] Leemans W P, Nagler B, Gonsalves A J, Tóth C, Nakamura K, Geddes C G R, Easrey C B and Hooker S M 2006 *Nat. Phys.* **2** 696
[3] Bartels R, Backus S, Zeek E, Misoguti L, Vdovin G, Christov I P, Murnane M M and Kapteyn H C 2000 *Nature* **406** 164
[4] Umstadter D 2001 *Phys. Plasmas* **8** 1774
[5] Emma P, Akre R, Arthur J, Bionta R, Bostedt C, Bozek J, Brachmann A, Bucksbaum P, Coffee R, Decker F J et al 2010 *Nat. Photon.* **4** 641
[6] Milburn R H 1963 *Phys. Rev. Lett.* **10** 75
[7] Kaplan A E and Shkolnikov P L 2002 *Phys. Rev. Lett.* **88** 074801
[8] Lan P F, Lu P X, Cao W and Wang X L 2005 *Phys. Rev. E* **72** 066501
[9] Schwoerer H, Liesfeld B, Schlenvoigt H P, Amthor K U and Sauerbrey R 2006 *Phys. Rev. Lett.* **96** 014802
[10] Glenzer S H and Redmer R 2009 *Rev. Mod. Phys.* **81** 1625
[11] Chen S, Powers N D, Ghebregziabher I, Maharjan C M, Liu C, Golovin G, Banerjee S, Zhang J, Cunningham N, Moorti A, Clarke S, Pozzi S and Umstadter D P 2013 *Phys. Rev. Lett.* **110** 155003
[12] Sarri G, Corvan D J, Schumaker W, Cole J M, Piazza A D, Ahmed H, Harvey C, Keitel C H, Krushelnick K, Mangles S P D, Najmudin Z, Symes D, Thomas A G R, Yeung M, Zhao Z and Zepf M 2014 *Phys. Rev. Lett.* **113** 224801
[13] Yan W C, Fruhling C, Golovin G, Haden D, Luo J, Zhang P, Zhao B Z, Zhang J, Liu C, Chen M, Chen S Y, Banerjee S and Umstadter D 2017 *Nat. Photon.* **11** 514
[14] Salamin Y I and Faisal F H M 1998 *Phys. Rev. A* **58** 3221
[15] Salamin Y I 1999 *Phys. Rev. A* **60** 3276
[16] Faisal F H M and Salamin Y I 1999 *Phys. Rev. A* **60** 2505
[17] Salamin Y I and Faisal F H M 2000 *Phys. Rev. A* **61** 043801
[18] Salamin Y I, Faisal F H M and Keitel C H 2000 *Phys. Rev. A* **62** 053809
[19] He F, Lau Y Y, Umstadter D P and Strickler T 2002 *Phys. Plasmas* **9** 4325
[20] Lau Y Y, He F, Umstadter D P and Kowalczyk R 2003 *Phys. Plasmas* **10** 2155
[21] He F, Lau Y Y, Umstadter D P and Kowalczyk R 2003 *Phys. Rev. Lett.* **90** 055002
[22] Lan P F, Lu P X and Cao W 2007 *Plasma. Sci. Technol.* **9** 143
[23] Fu Y J, Jiang C, Lv C, Wan F, Sang H B and Xie B S 2016 *Phys. Rev. A* **94** 052102
[24] Jiang C, Xie H Z, Sang H B and Xie B S 2017 *Europhys. Lett.* **117** 44002
[25] Li J, Xie B S, Sang H B, Hong X R, Zhang S and Yu M Y 2009 *Appl. Phys. Lett.* **95** 161105
[26] Jackson J D 1975 *Classical Electrodynamics* (New York: Wiley)